IUBMB *Life*, 50: 99–103, 2000

1521-6543/00 $12.00 + .00

Original Research Article

Dual Effect of Nucleotides on P2Y Receptors

Katrin Sak,[1] Eric A. Barnard,[2] and Jaak Järv[1]
[1] *Institute of Chemical Physics, Tartu University, 2 Jakobi Street, 51014 Tartu, Estonia*
[2] *Department of Pharmacology, University of Cambridge, Tennis Court Road, Cambridge, CB2 1QJ, U.K.*

Summary

The interaction of ADP, 2MeSADP, and ADPβS with the adenine nucleotide receptor $P2Y_1$ in the $hP2Y_1$-1321N1 cell line and of UDP with a receptor or receptors recognizing pyrimidine nucleotides in NG108-15 cells was studied over a wide range of ligand concentrations. Bell-shaped dose–response curves for stimulation of phosphoinositide hydrolysis were obtained in these cells. This dual behavior of the agonists studied was characterized by two dissociation constants, K_{agon} and K_{antag}, which quantify the agonistic and antagonistic activity of these ligands and can be compared with the conventional EC_{50} and IC_{50} values, respectively. The data revealed a common pattern of agonistic and antagonistic behavior of nucleoside diphosphates and their derivatives at these two types of P2Y receptors, pointing to some similar properties of their nucleotide binding sites.

IUBMB *Life*, 50: 99–103, 2000

Keywords Dual effect; inositol phospholipid hydrolysis; nucleoside diphosphate; P2Y receptor.

INTRODUCTION

The G-protein–coupled P2Y receptors belong to the class of 7-transmembrane domain (7-TM) proteins, so far, 9 subtypes of these nucleotide receptors have been found in vertebrates by DNA cloning (*1*, *2*). These receptors reveal substantial structural homology with other 7-TM receptors (*3*), which, in turn, suggests the possibility of similar functional aspects. In this report we have examined the ability of the P2Y receptors to produce the bell-shaped dose–response curves previously observed with some other G-protein–coupled receptors, a finding most thoroughly analysed for muscarinic receptor–regulated cAMP synthesis (*4*) and for the mobilisation of intracellular Ca^{2+} by muscarinic agonists (*5*). The dual effect of nucleotides was observed for both a purine-specific and a pyrimidine-specific receptor. To minimise uncertainties related to the decomposition of nucleoside triphosphates during the assay procedure (*6*), only nucleoside diphosphates and their structural analogues were used in this analysis, given that the corresponding monophosphates and nucleosides are known to be (*1*, *2*) at best very weak ligands for any of these receptors.

Received 11 February 2000; accepted 3 July 2000.
Address correspondence to Jaak Järv. E-mail: jj@chem.ut.ee

EXPERIMENTAL PROCEDURES

Chemicals. UDP, ADP, AMP, and adenosine were obtained from Boehringer Mannheim; UMP, uridine, 2MeSADP, and ADPβS were from Sigma. The purity of all these compounds was analysed before their use by HPLC (Gilson) on an anion-exchange column Mono Q (Pharmacia Biotech). Absorbance was monitored at 258 nm for adenine nucleotides and at 270 nm for uracil nucleotides. Linear gradients from 0 to 1 M NaCl in 40 mM phosphate buffer (pH 7.0) and from 0.1 to 1.2 M ammonium carbonate in water at the flow rate 1 ml/min were used. If necessary, the nucleotides were additionally purified by rechromatographing with the latter gradient. The purity of nucleotides in the assay was never <99.5%, and no corresponding triphosphates were detected in the samples used. *myo*-[2-^{3}H]Inositol was purchased from Amersham.

Cell Cultures. NG108-15 cells were obtained from the European Collection of Cell Cultures (no. 88112302). $hP2Y_1$-1321N1 cells were the stable cell line expressing the human $P2Y_1$ receptor, as described elsewhere (*7*). Both cell types were cultured in Dulbecco's modified Eagle's medium (DMEM; Gibco) supplemented with 10% (v/v) fetal calf serum and tylosine (8 μg/ml). For NG108-15 cells the medium was further supplemented with 0.1 mM hypoxanthine, 1 μM aminopterin, and 16 μM thymidine. The medium for $hP2Y_1$-1321N1 cells was supplemented with 400 μg/ml G-418 sulfate (Gibco BRL). Cells were grown at 37 °C in a humidified atmosphere of 95% air and 5% CO_2 in 75-cm^2 culture dishes.

Assay of Inositol Phosphates. Cells were seeded on 24-well culture plates at a density of $\sim 5 \times 10^4$ cells/well for NG108-15 and $\sim 1 \times 10^5$ cells/well for $hP2Y_1$-1321N1 and grown to

subconfluence for 3 days. [^{3}H]-Inositol was added to the cells in 200 μl of inositol-free DMEM at 2 μCi/ml 18 h before the assay. No changes in medium were made subsequent to [^{3}H]inositol addition. The ligands were added in 50 μl of 50 mM LiCl and 100 mM phosphate buffer (pH 7.2), and the assay mixture was incubated 10 min at 37 °C. A check of the pH of the assay medium after the assay indicated no systematic change, even at high ligand concentrations.

The assay was terminated by aspirating the medium and adding 0.5 ml of ice-cold 5% trichloroacetic acid. The resulting supernatant was extracted three times with 0.5 ml of diethyl ether and inositol phosphates were isolated on the Dowex AG1-×8 columns (Bio-Rad; 100–200 mesh, formate form, bed volume 0.8 ml). These columns were washed with water (2 × 4 ml) and 50 mM ammonium formate (8 ml); inositol phosphates were eluted with 1 M ammonium formate in 0.1 M formic acid (2 × 4 ml). The amount of [^{3}H]inositol phosphates formed was determined by adding scintillation cocktail (OptiPhase HiSafe III; Wallac) to each eluate and counting the radioactivity present. Under the experimental conditions used the baseline radioactivity of the samples remained between 600 and 700 cpm/sample. The maximal radioactivity measured during the assay time was 2700–2900 cpm/sample for NG108-15 cells and 3200–3400 cpm/sample for hP2Y$_1$-1321N1 cells. When investigating the time-dependence of accumulation of the inositol phosphates, incubation times between 3 and 20 min were used.

Data Processing. The bell-shaped dose–response curves were analysed by assuming that the interaction of a ligand A at the agonistic and antagonistic receptor sites follows the mass action law and that relative effect can be presented as a combination of two binding isotherms (*8*):

$$\text{Relative effect} = \frac{[A]}{K_{agon} + [A]} - \frac{[A]}{K_{antag} + [A]} \qquad [1]$$

The parameters K_{agon} and K_{antag} have the meaning of the appropriate dissociation constants and can be compared with the concentrations at which one-half of binding is complete or inhibited (conventional EC_{50} and IC_{50} values), respectively. Experimental data were expressed in semilogarithmic coordinates (Fig. 1) by means of a nonlinear regression analysis program Prism^{TM} (ver. 2.00), and the calculated parameters were reported with standard errors (±SE). The number of experiments used in calculations corresponded to the number of points shown in Fig. 1.

RESULTS

Effect of ADP and Its Derivatives on the Human P2Y$_1$ Receptor Stably Expressed in Astrocytoma 1321N1 Cells

ADP, 2MeSADP, and ADPβS induced the synthesis of inositol phosphates in hP2Y$_1$-1321N1 cells, whereas uracil nucleotides were inactive therein. With ADP the time-dependence of formation of inositol phosphates was analysed. During the first 20 min the increase in product concentration was linear (Fig. 2A), in agreement with the assumptions that no significant degradation of the ligand occurred during the assay, and the initial rate of the process was measured. Indeed, separate chromatographic analysis revealed that only 5–10% of ADP was converted into AMP in the assay medium during 10 min.

The dose–response curves for ADP, 2MeSADP, and ADPβS were measured at ligand concentrations from 0.1 nM to 10 mM. At millimolar concentrations all these compounds caused a clear downturn of the dose–response curves, pointing to inhibition of the response at high ligand concentration (Fig. 1A–C). The data were analysed by using Eq. 1, and the pK_{agon} and pK_{antag} values were calculated (Table 1). These constants varied for different ligands, but the maximum response evoked by all the agonists was equal. Secondly, the results were independent on the length

Table 1
Effect of nucleoside diphosphates and their analogues on synthesis of inositol phosphates in hP2Y$_1$-1321N1 and NG108-15 cells at various concentrations of divalent ions

	Assay conditions				
Nucleotide	[Ca^{2+}] (mM)	[Mg^{2+}] (mM)	EDTA (mM)	pK_{agon}	pK_{antag}
hP2Y$_1$-1321N1 cells					
ADP	1.80	0.813	—	7.2 ± 0.1	2.1 ± 0.1
	1.80	10.00	—	5.9 ± 0.1	1.6 ± 0.1
	—	—	4.00	6.8 ± 0.1	2.0 ± 0.1
2MeSADP	1.80	0.813	—	7.8 ± 0.1	2.9 ± 0.1
ADPβS	1.80	0.813	—	6.4 ± 0.1	1.8 ± 0.2
NG108-15 cells					
UDP	1.80	0.813	—	6.4 ± 0.1	1.8 ± 0.1
	1.80	10.00	—	6.1 ± 0.1	2.0 ± 0.2
	—	—	4.00	6.4 ± 0.1	2.0 ± 0.3

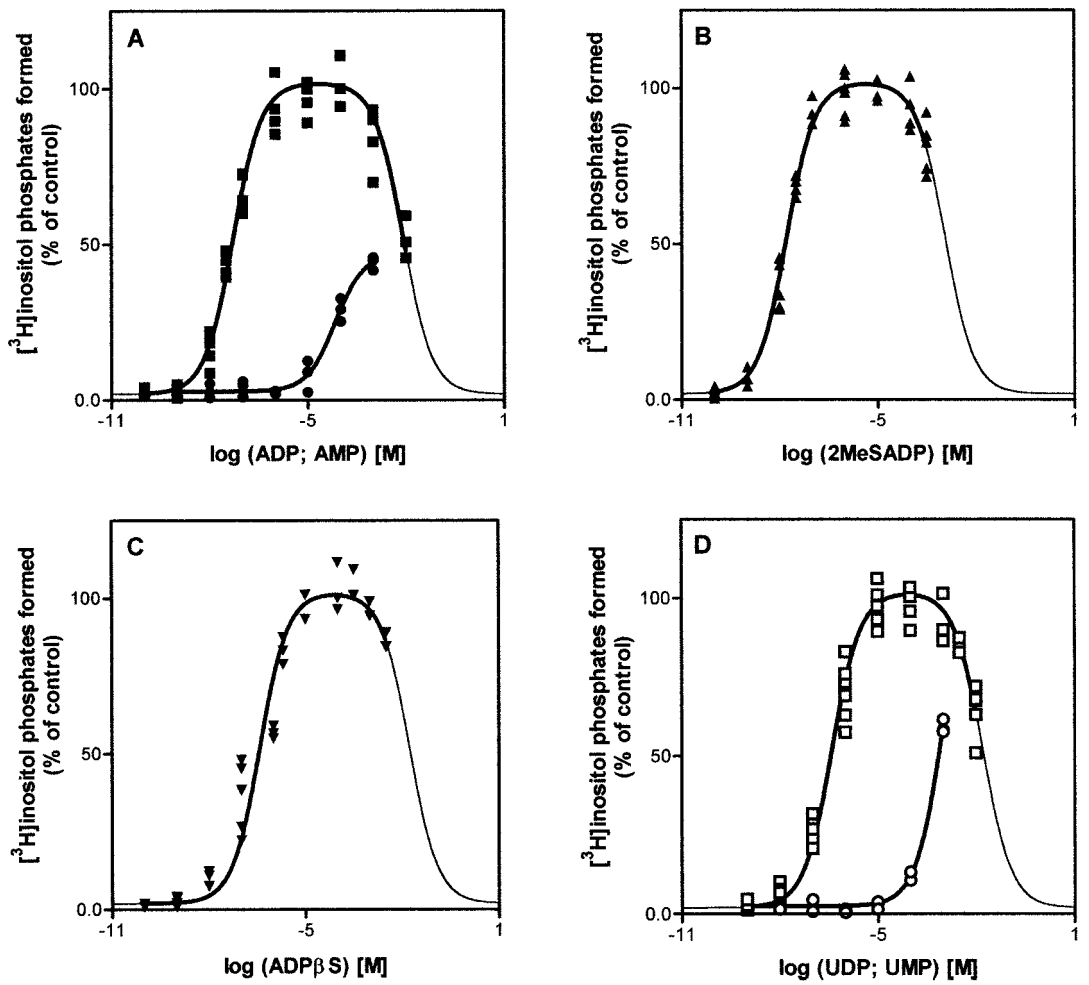

Figure 1. Effect of ADP (A, ■), AMP (A, ●), 2MeSADP (B), and ADPβS (C) on the hP2Y$_1$ expressed in 1321N1 cells and the effect of UDP (D, □) and UMP (D, ○) on the pyrimidinergic receptor or receptors expressed by NG108-15 cells.

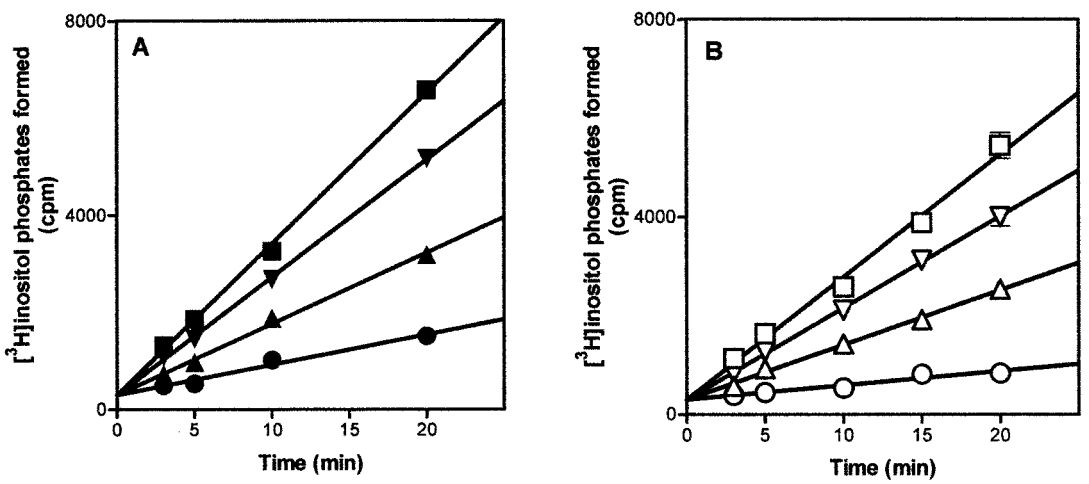

Figure 2. Time dependence of the accumulation of inositol phosphates. The values are the means ±SEM of triplicate determinations in 2 independent experiments. (A) hP2Y$_1$-1321N1 cells were incubated with 50 μM (■), 5 μM (▼), 500 nM (▲), or 50 nM (●) ADP. (B) NG108-15 cells were incubated with 100 μM (□), 10 μM (▽), 1 μM (△), or 100 nM (○) UDP.

of the incubation time, as shown by the linear time dependence of formation of inositol phosphates (Fig. 2A).

In parallel, the influence of AMP and adenosine was tested with $hP2Y_1$-1321N1 cells. AMP had only a weak effect (Fig. 1A), whereas adenosine and the uracil nucleotides, including UDP, clearly had no effect in this system. At 1 mM, neither AMP nor adenosine produced any antagonist change in the 2MeSADP curve.

Effect of UDP on Pyrimidinoceptor(s) Expressed by NG108-15 Cells

In the NG108-15 cell line, the synthesis of inositol phosphates was activated by UDP, whereas the adenine nucleotides used above had only a minor effect on this process. The NG108-15 cells express $P2Y_1$, $P2Y_2$, and $P2Y_6$ but not $P2Y_4$, as determined by polymerase chain reaction analysis (*6*). Because UDP is inactive on $P2Y_1$ (*9*) and $P2Y_2$ (*10*), we presume that the response to UDP (*11*) occurs through the $P2Y_6$ receptor, although a contribution from some other undetected and unknown subtype cannot be excluded.

The time dependence of the UDP-initiated formation of inositol phosphates was found to be linear in these cells for at least 20 min (Fig. 2B), so again the time interval of 10 min was used in all receptor assays. The dose–response curve for UDP was monitored with NG108-15 cells at concentrations from 0.1 nM to 10 mM. Within this concentration interval, the plot revealed a clear bell-shaped form (Fig. 1D), and the values of pK_{agon} and pK_{antag} were calculated, as listed in Table 1. Under the same experimental conditions, UMP had only a weak effect on the synthesis of inositol phosphates, with $EC_{50} = 1.0 \pm 0.6$ mM (Fig. 1D), whereas uridine had no effect at 1 mM concentration. At 1 mM, neither UMP nor uridine had an antagonist effect on the UDP response.

Effect of Mg^{2+} and Ca^{2+} Ions and EDTA on Synthesis of Inositol Phosphates

The concentration of Mg^{2+} and Ca^{2+} ions was varied in the assay mixture to analyse the possible role of the nucleotide–ion complexes in formation of the receptor response. For both cell lines the concentration of Mg^{2+} in the assay medium was increased from 0.8 to 10 mM. In other experiments divalent metal ions were omitted from the assay medium and 4 mM EDTA was added. Under these rather extreme conditions, the dose–response curves were still bell-shaped and described by Eq 1, yielding the dissociation constants pK_{agon} and pK_{antag} close to the values obtained under the routine assay conditions (Table 1). On the other hand, the maximal rate of synthesis of inositol phosphates in both cell lines was affected under these conditions. For example, in the presence of 10 mM Mg^{2+} the ADP- and UDP-induced maximal responses were 1.8 and 2.2 times more than the maximal effect obtained under the standard assay conditions; in the absence of the divalent metal ions, however, about half of the standard response was observed.

DISCUSSION

The receptors, expressed by $hP2Y_1$-1321N1 and NG108-15 cells, revealed clear selectivity against adenine and uracil nucleotides, respectively. This along with the EC_{50} values listed in Table 1, is in good agreement with most of the results published for these cells (receptor subtypes) and collected in the P2Y Receptor Ligand Database, available on the Internet (http://bioorg.chem.ut.ee/p2y/).

On the other hand, at high ligand concentrations a clear downturn in the dose–response curves was observed (Fig. 1), leading to a nonconventional bell-shaped plot and pointing to the dual nature of action of agonists on the purine-selective and pyrimidine-selective receptors studied.

We excluded the obvious potential artefact of an antagonist impurity, which becomes significant in size only when high ligand concentrations are applied. First, the purity of agonists was checked before their use in experiments. Second, there was no change in the pK_{agon} and pK_{antag} values when EDTA was added to an amount that would complex polyvalent metal impurities in general. Third, the processing of a diphosphate by *ecto*-enzymes was shown to be low during the assays, and even for that low conversion level, the main product from ADP was AMP, which is itself a weak agonist (Fig. 1A) on these cells and therefore irrelevant to this question.

The dual effect of specific agonists at the G-protein–coupled 7-TM receptors and the formation of the bell-shaped dose–response curves can be explained by at least two theoretical models. The first model involves interaction of the same agonist with two distinct receptor populations, which have different affinities for the ligand and produce opposite effects (*12*). The second model assumes that the stimulatory (agonistic) and inhibitory (antagonistic) effects of the same drug can be related to the presence of two distinct ligand-binding sites on the receptor molecule, which are responsible for signal transduction (agonistic site) and inhibition (antagonistic site), respectively (*8*). In both models, the difference between agonistic and antagonistic effects of a ligand is determined by differences in specificity of the appropriate binding sites, and even the parameters calculated from the bell-shape dose–response curve have quite similar meanings.

According to the two-site receptor model (*8*), the dissociation constant K_{antag} should characterise the antagonistic receptor sites. In the case of the P2Y receptor subtypes, the binding properties of these sites are still not clearly understood, because only a few and usually nonspecific antagonists have been described. Therefore, the analysis of the bell-shaped dose–response curves seems to provide a method for characterisation of the specificity patterns of the antagonistic sites on purinergic and pyrimidinergic receptor subtypes. The affinities there are very weak, but the effect of those sites nevertheless becomes discernible at diphosphate concentrations $>10\ \mu$M (Fig. 1).

Recent molecular modelling studies on the human $P2Y_1$ receptor structure has revealed the possibility of ATP binding to at least two distinct domains of the receptor molecule (*13*). One

of these domains was proposed to be located outside of the TM segments and was formed by the extracellular loops 2 and 3, whereas the other proposed binding domain was located within the TM core. The former binding was calculated to be weaker and was hypothesised to function to move an ATP molecule into the functional strong binding site (*13*). These domains may well correspond to the agonistic and antagonistic sites predicted by the two-site receptor model.

The theoretical analysis of muscarinic receptor interaction with specific ligands has also suggested distinct locations of agonist (carbachol) and antagonist (*N*-methylscopolamine) molecules on the receptor (*14*). Given that variations of structure of classical muscarinic agonists and antagonists have revealed rather different structure–activity relationships for these ligands, the appropriate binding sites should possess different patterns, thereby explaining the existence of very potent and highly selective ligands of both types of activity (*15*).

On the other hand, the data listed in Table 1 reveal that variation in ligand structure resulted in rather similar changes in K_{agon} and K_{antag} for the nucleotides. Thus the putative binding sites on the P2Y receptors seem to possess rather close specificity patterns, presumably dominated by the phosphate groups. This may be one of the reasons why the discovery of selective and potent antagonists for these receptors has been elusive for so long. We hope that this information about the putative antagonistic sites may be useful for development of these studies.

ACKNOWLEDGEMENT

This work was supported by the EU Inco-Copernicus Grant IC 15-CT96-0919 (DG 12-CDPE), and by the Wellcome Trust. We thank Külli Samuel (Institute of Chemical Physics and Biophysics, Tallinn, Estonia) for cultivation of the cells and Gerda Raidaru (Institute of Chemical Physics, Tartu, Estonia) for chromatographic analysis of nucleotides.

REFERENCES

1. Barnard, E. A., Simon, J., and Webb, T. E. (1997) Nucleotide receptors in the nervous system. An abundant component using diverse transduction mechanisms. *Mol. Neurobiol.* **15**, 103–129.
2. Ralevic, V., and Burnstock, G. (1998) Receptors for purines and pyrimidines. *Pharmacol. Rev.* **50**, 413–492.
3. Barnard, E. A. (1997) Protein structures in receptor classification. *Ann. N.Y. Acad. Sci.* **812**, 14–28.
4. Järv, J., Toomela, T., and Karelson, E. (1993) Dual effect of carbachol on the muscarinic receptor. *Biochem. Mol. Biol. Int.* **30**, 649–654.
5. Järv, J., Hautala, R., and Åkerman, K. E. O. (1995) Dual effect of muscarinic receptor agonists on Ca^{2+} mobilization in SH-SY5Y neuroblastoma cells. *Eur. J. Pharmacol.* **291**, 43–50.
6. Webb, T. E., and Barnard, E. A. (1999) Molecular biology of P2Y receptors expressed in the nervous system. *Prog. Brain Res.* **120**, 23–31.
7. Ayyanathan, K., Webb, T. E., Sandhu, A. K., Athwal, R. S., Barnard, E. A., and Kunapuli, S. P. (1996) Cloning and chromosomal localization of the human P2Y1 purinoceptor. *Biochem. Biophys. Res. Commun.* **218**, 783–788.
8. Järv, J. (1995) A model of non-exclusive binding of agonist and antagonist on G-protein coupled receptors. *J. Theor. Biol.* **175**, 577–582.
9. Simon, J., Webb, T. E., King, B. F., Burnstock, G., and Barnard, E. A. (1995) Characterisation of a recombinant P2Y purinoceptor. *Eur. J. Pharmacol.* **291**, 281–289.
10. Nicholas, R. A., Watt, W. C., Lazarowski, E. R., Li, Q., and Harden, T. K. (1996) Uridine nucleotide selectivity of three phospholipase C-activating P2 receptors: identification of a UDP-selective, a UTP-selective, and an ATP-and UTP-specific receptor. *Mol. Pharmacol.* **50**, 224–229.
11. Sak, K., Webb, T. E., Samuel, K., Kelve, M., and Järv, J. (1999) Only pyrimidinoceptors are functionally expressed inmouse neuroblastoma cell lines. *Mol. Cell Biol. Res. Commun.* **1**, 203–208.
12. Szabadi, E. (1977) A model of two functionally antagonistic receptor populations activated by the same agonist. *J. Theor. Biol.* **69**, 101–112.
13. Moro, S., Hoffmann, C., and Jacobson, K. A. (1999) Role of the extracellular loops of G protein-coupled receptors in ligand recognition: a molecular modeling study of the human P2Y1 receptor. *Biochemistry* **38**, 3498–3507.
14. Fanelli, F., Menziani, M. C., and Benedetti, P. G. (1995) Molecular dynamics simulations of m3-muscarinic receptor activation and QSAR analysis. *Bioorg. Med. Chem.* **11**, 1465–1477.
15. Järv, J. (1992) Neurotoxic agents interacting with the muscarinic acetylcholine receptor. In *Handbook of Experimental Pharmacology, vol. 102, Selective Neurotoxicity* (Herken, H., and Hucho, F., eds), pp. 659–680, Springer-Verlag, Berlin.